Lab-on-a-disc agglutination assay for protein detection by optomagnetic readout and optical imaging using nano- and micro-sized magnetic beads

Uddin, Rokon; Burger, Robert; Donolato, Marco; Fock, Jeppe; Creagh, Michael; Hansen, Mikkel Fougt; Boisen, Anja

Published in:
Biosensors and Bioelectronics

Link to article, DOI:
10.1016/j.bios.2016.05.023

Publication date:
2016

Document Version
Peer reviewed version

Lab-on-a-disc agglutination assay for protein detection by optomagnetic readout and optical imaging using nano- and micro-sized magnetic beads

Rokon Uddin[a*], Robert Burger[b], Marco Donolato[b], Jeppe Fock[a], Michael Creagh[b], Mikkel Fougt Hansen[a] and Anja Boisen[a]

[a]Department of Micro- and Nanotechnology, Technical University of Denmark, DTU Nanotech, Building 345 East, DK-2800 Kongens Lyngby, Denmark

[b]BluSense Diagnostics, Fruebjergvej 3, DK-2100 Copenhagen Ø, Denmark

*Corresponding author: Rokon Uddin
Contact: Ørsteds Plads, Building 345C, 110
2800 Kgs. Lyngby, Denmark
Tel: +4545256343
Email: rokud@nanotech.dtu.dk

Abstract

We present a biosensing platform for the detection of proteins based on agglutination of aptamer coated magnetic nano- or microbeads. The assay, from sample to answer, is integrated on an automated, low-cost microfluidic disc platform. This ensures fast and reliable results due to a minimum of manual steps involved. The detection of the target protein was achieved in two ways: (1) optomagnetic readout using magnetic nanobeads (MNBs); (2) optical imaging using magnetic microbeads (MMBs). The optomagnetic readout of agglutination is based on optical measurement of the dynamics of MNB aggregates whereas the imaging method is based on direct visualization and quantification of the average size of MMB aggregates. By enhancing magnetic particle agglutination via application of strong magnetic field pulses, we obtained identical limits of detection of 25 pM with the same sample-to-answer time (15 min 30 s) using the two differently sized beads for the two detection methods. In both cases a sample volume of only 10 µl is required. The demonstrated automation, low sample-to-answer time and portability of both detection instruments as well as integration of the assay on a low-cost disc are important steps for the implementation of these as portable tools in an out-of-lab setting.

Keywords: Magnetic bead, agglutination assay, thrombin, microfluidic disc, optomagnetic readout method, optical imaging method

1. Introduction

Magnetic nano- and microbeads are being widely used for sensing of various biomolecules in different microfluidic systems (Antunes *et al.*, 2015) Kwakye *et al.*, 2006; Steigert *et al.*, 2005; Wang *et al.*, 2013; Zaytseva *et al.*, 2005; Choi *et al.*, 2002). Magnetic beads (MBs) can be utilized for detection of pathogens (Mezger *et al.*, 2015; Beyor *et al.*, 2008; El-Boubbou *et al.*, 2007; Gu *et al.*, 2006; Song *et al.*, 2013; Zaytseva *et al.*, 2005), small molecules (Yang *et al.*, 2016; Wu *et al.*, 2011; Zhang *et al.*, 2013) and proteins (Nam *et al.*, 2003 ; Tsai *et al.*, 2007; Horng *et al.*, 2006), for drug delivery (Chertok *et al.*, 2008; Gonzales and Krishnan, 2005; Jain *et al.*, 2008; Wilson *et al.*, 2005), and even for testing certain characteristics of a drug (Quan *et al.*, 2015). Due to the weak magnetic properties of biomolecules, a readout based on magnetic beads (MBs) is insensitive to chemical and biological parameters that may affect other readout techniques and is thus highly attractive (Yang *et al.*, 2016; Bejhed *et al.*, 2015; Hecht *et al.*, 2013). In addition, due to the simple readout, the detection devices can be produced at a low cost, facilitating their usage in resource-limited settings (Yager *et al.*, 2008).

Assays based on agglutination of MBs, i.e., the formation of MB clusters in order to detect biomarkers, are being widely studied due to the simplicity of the readout (Donolato *et al.*, 2015; Göransson *et al.*, 2010; Ranzoni *et al.*, 2012; Wang and Gan, 2009). In these assays, the beads are coated with molecules with specific affinity to bind a target

molecule. The presence of the target molecule causes the MBs to bind together to form aggregates of different sizes and shapes. Based on the physical characteristics of the aggregates as well as their rotational dynamics in response to an external oscillating magnetic field, the concentration of the target molecule can be determined. Magnetic bead-based agglutination assays are promising for point-of-care (POC) diagnostics.

However, in several studies of agglutination assays using magnetic beads, the use of complex microfluidics, sophisticated readout methods, large sample volume and lack of automation have limited their real point-of-care potential. For instance, Chen *et al.*, 2013 developed a microfluidic chip-based assay using aptamer-functionalized magnetic beads labelled with fluorescent dye Cy3 for detecting thrombin. 50 µl of biotinylated Aptamer II labelled with Cy3 was incubated with 50 µl thrombin solution for 30 min. Aptamer I functionalized with magnetic beads was then loaded into the chip through external tubing. Since the chip was placed under a permanent magnet, the aptamer-functionalized beads were aggregated. Subsequently, aptamer II labelled with Cy3 and functionalized with thrombin was loaded into the chip to react with aptamer I. Finally, any unreacted aptamer II was washed out using an external syringe pump followed by fluorescent measurement with a microarray scanner. Thus, the whole process involved large assay time, multiple manual steps and external components.

Tennico *et al.*, 2010 performed a similar study on a further developed chip, but used quantum dot nanocrystals instead of Cy3 dye and integrated a nanoport on the chip to connect with external syringe pump for washing in an automated fashion resulting in less reagent consumption and a shorter reaction time. The steps of the assay included: loading of 3 µl aptamer I functionalized with magnetic beads into reaction chamber followed by magnetic bead aggregation by on-chip magnets, rinsing of excess aptamers using external syringe pump, addition of 3 µl of thrombin solution into the reaction chamber followed by 5 min incubation period, rinsing and washing with binding buffer, addition of 6 µl aptamer II labelled with quantum dot nanocrystals into reaction chamber followed by further 5 min incubation, and finally a last washing step before measurement by a fluorescent microscope. Although the sample consumption and assay time was reduced compared to that presented in Chen *et al.*, 2013, it still suffered from the limitations imposed by use of syringe pump as well as multiple assay steps including washing and rinsing, which makes it difficult to use it in an out-of-lab setting.

Finally, a magnetic microbead-based fluorescent-independent agglutination assay using the same aptamers as used in the above-mentioned studies for detecting thrombin in buffer solution was reported by Hecht *et al.*, 2013. The rotational period of the formed aggregates as well as their shape, size and fractal dimension were measured to quantify the concentration of thrombin. There, the sample-to-answer time was more than 40 min and the assay required multiple manual steps.

Here, we present a conventional sandwich agglutination assay for detection of the model protein thrombin in buffer (Hecht *et al.*, 2013), but the assay steps are integrated and automated on a low-cost microfluidic disc. As a significant achievement, thanks to the introduction of an on-disc magnetic field assisted incubation protocol (Antunes *et al.*, 2015), we reduce the sample-to-result time from 40 min to 15 min 30 s while utilizing only 10 µl of sample. We verify that an optimum incubation of the samples with magnetic beads under magnetic field, hereafter termed 'magnetic incubation', effectively enhances the MB agglutination (Antunes *et al.*, 2015; Ranzoni *et al.*, 2012; Baudry *et al.*, 2006) and results in fast detection. By utilizing the magnetic incubation protocol, we detect different concentrations of thrombin based only on the size distribution of MB aggregates.

We validate the lab-on-a-disc agglutination assay for both micro (1 µm) and nano (100 nm)-sized magnetic beads. We use two different detection methods for the MNB and MMB-based assays. The detection method used for MNB-based assay is the previously presented optomagnetic readout method (Mezger *et al.*, 2015; Bejhed *et al.*, 2015; Donolato *et al.*, 2015). The optomagnetic setup (Donolato *et al.*, 2015) uses a Blu-ray optical pickup unit (OPU) as the excitation element and a photodetector as the sensing element. An AC magnetic field excitation is provided by an off-chip electromagnet. The frequency-dependent modulation of the optical transmission signal correlates with the hydrodynamic size of the MNB aggregates and enables a sensitive and quantitative detection of a target molecule based on the aggregate size (Donolato *et al.*, 2015).

The detection method used for the MMB-based assay is an optical imaging method that detects the area of particle aggregates formed due to the presence of thrombin by fast direct imaging. We use a commercial imaging and scanning instrument 'oCelloScope' (Philips BioCell), which combines the optical sectioning principle of confocal microscopy with an automated scanning principle. A detailed description of the oCelloScope setup can be found in

(Fredborg *et al.*, 2013) and in the Supplementary Material Section S2. The automation, user-friendliness, fast detection and portability of both detection instruments along with the integration of the assay steps on the disc make both systems strong candidates for a simple sample-to-answer device for use in an out-of-lab setting.

2. Experimental

2.1 Materials and Chemicals

The assay platform in this work is a microfluidic disc. Each disc (thickness: 2 mm) contains eight microfluidic units each with three inlet chambers, a mixing/measuring chamber and a pneumatic chamber for ensuring pneumatic mixing (Figs. 1a, b). The disc was fabricated from three layers of Polymethylmethacrylate (PMMA) bonded by pressure sensitive adhesive (PSA) in less than 20 min. The detailed fabrication procedure of the disc is presented in (Donolato *et al.*, 2015) and in the Supplementary Material Section S1.

The MBs used in this study are streptavidin coated beads with diameters of 100 nm and 1 μm, respectively. The particular bead size was chosen as previous studies showed that the optomagnetic signal is more sensitive to formation of aggregates when the MNB size is about 100 nm (Donolato *et al.*, 2015; Yang *et al.*, 2016); and the 1 μm bead size was reported as optimum for MMBs based on sedimentation rate and available binding sites (Hecht *et al.*, 2013), making it an ideal candidate for the optical imaging study. The MNBs were purchased from Micromod (Micromod Partikeltechnologie GmbH, Rostock, Germany). The MMBs (T1 Dynabeads) as well as the human alpha thrombin (product code T6884) were purchased from Sigma-Aldrich. Three different buffer solutions were prepared for washing, aptamer binding and thrombin binding, the details of which are provided in Supplementary Material Section S1. Two widely used anti-thrombin aptamers functionalized with 5` biotin and consisting of 29-mer and 15-mer with 20 base poly-T tails (Table 1) were purchased from DNA technology (Denmark). We have used these two particular aptamers because of their well-proven specificity to bind with thrombin molecule (Bock *et al.*, 1992; Tasset *et al.*, 1997).

Table1: Sequence of thrombin-binding aptamers used in study

Aptamer	Sequence
15-mer DNA aptamer	5´-Biotin-TTT TTT TTT TTT TTT TTT TT GGT TGG TGT GGT TGG-3´
29-mer DNA aptamer	5´-Biotin-TTT TTT TTT TTT TTT TTT TT AGT CCG TGG TAG GGC AGG TTG GGG TGA CT-3´

2.2 Magnetic bead functionalization

We prepared two sets of aptamer-functionalized MBs, one for nano-sized beads and the other for micro-sized beads. An aliquot of 10 μl of streptavidin-coated MNBs (10 mg/ml) was washed three times with the washing buffer, resuspended in 100 μl of aptamer-binding buffer and subsequently split into two equal aliquots (Hecht *et al.*, 2013). 4 μl of 50 μM biotinylated aptamer solution (each of 29-mer or 15-mer) was added to each aliquot and incubated for 45 min at room temperature to functionalize the beads with the specific aptamers by forming the biotin-streptavidin bonds. The MNB solution was then washed three times with thrombin-binding buffer and finally resuspended at a bead concentration of 0.1 mg/ml (Antunes *et al.*, 2015). The same protocol was followed for functionalizing the MMBs.

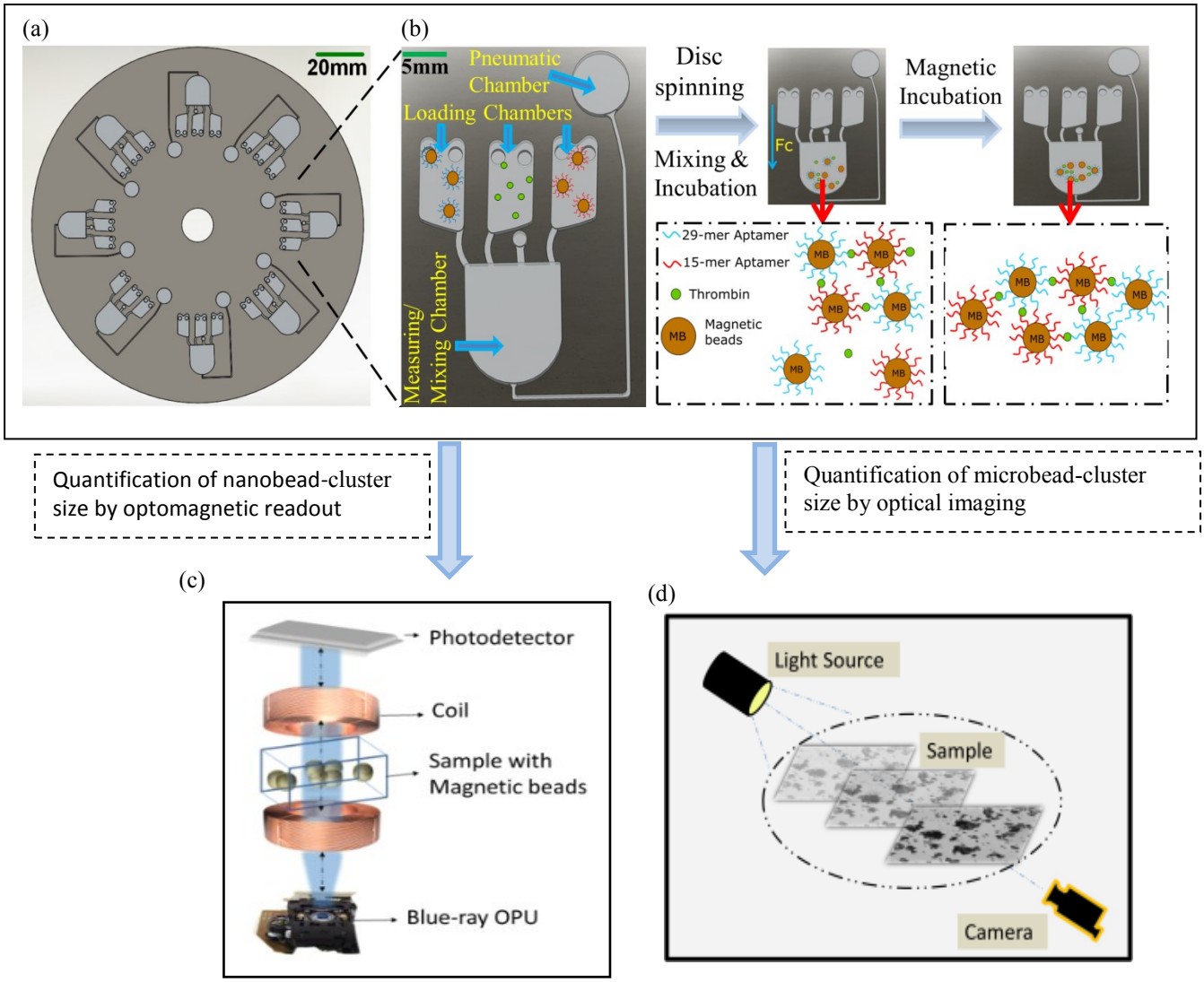

Fig.1: (a) Schematic of the microfluidic disc with eight repeating functional units. (b) Illustration of one of the functional repeating units of the disc indicating different chambers followed by MB aggregation formation due to the presence of thrombin. (c) Schematic of the functional unit of the optomagnetic readout method for quantifying the nanobead cluster size (Supplementary Material Section S2). (d) Schematic of the functional unit of optical imaging method for quantifying the microbead cluster size (Supplementary Material Section S2).

2.3 Experimental procedure

An aptamer-based agglutination assay was used for thrombin detection. The aptamers used in this study have the specific affinity to bind to two structurally opposite sites of the thrombin molecule. The experimental procedure consisted in mounting the disc at the specific location of the optomagnetic setup followed by injecting aptamer-functionalized magnetic beads (MBs) (10 µl of each type) and thrombin solution (10 µl) into the three separate loading chambers of one of the microfluidic units of the disc (Fig. 1b). No pretreatments were made in the microfluidic units of the disc.

Spinning of the disc transferred the liquids of the loading chamber to the mixing/measuring chamber (Fig.1b). On-disc mixing of the liquids was performed by a pneumatic mixing routine for 30 s (Noroozi *et al.*, 2011). Subsequently, the solution was incubated on-disc at RT for 10 min in order to facilitate binding between the aptamers and the thrombin molecules. The incubation caused the formation of MB-aptamer-thrombin bonds, which resulted in

aggregation of MBs as illustrated in Fig. 1b. Subsequently, 5 min of magnetic incubation was performed to further stimulate and enhance MB agglutination. The magnetic incubation consisted of repeated cycles of two steps: (1) incubation in a strong magnetic field (60 mT) between two permanent magnets to promote formation of MB clusters; (2) mixing by shaking the disc to break unspecific bindings and to facilitate re-orientation of the beads (Antunes *et al.*, 2015). The magnetic incubation protocol was previously optimized in (Antunes *et al.*, 2015) for similar magnetic nanobeads. With a minor modification, we have employed this magnetic incubation protocol on both the nanobeads and the microbeads. Further information on the magnetic incubation protocol is provided in the Supplementary Material Section S2. Finally, after magnetic incubation, the MNB-based samples were measured by the optomagnetic readout method and the MMB-based samples were measured by the optical imaging method. For the optical imaging method, the disc was unmounted from the optomagnetic setup and transferred to the oCelloScope for scanning. The entire lab-on-a-disc agglutination assay including the time for incubation took 15 min 30 s while requiring only 10 µl of sample volume.

3. Results and Discussion

3.1 Time-lapse analysis without magnetic incubation

We first performed a time-lapse analysis without magnetic incubation for a specific concentration of thrombin (2 nM) to investigate the kinetics of the MB aggregation. For the time-lapse analysis by optical imaging of MMBs, the sample-filled measurement chamber was kept under the oCelloScope and scanned every 15 min using a routine-setup of the control software until the MMB aggregation saturated. Similarly, for the optomagnetic readout method using MNBs, time-lapse measurements were performed until signal saturation was observed in the optomagnetic spectra.

Fig. 2a shows the in-phase part of the normalized optomagnetic spectra (V_2'/V_0 vs. f) after incubation at the indicated times. Here, V_2' is the in-phase component of the 2nd harmonic of the transmitted light intensity with respect to the magnetic field excitation and V_0 is the average value of the transmitted light intensity. The signal increase at low frequencies that peaks near f = 7.5 Hz indicates the formation and growth of MNB aggregates over time due to the presence of thrombin. Fig. 2b shows the V_2'/V_0 -values at f = 7.5 Hz vs. time. The results indicate that the signal without magnetic incubation reached saturation after approximately 50 min.

Figs. 2c and 2d show optical images and the corresponding mean area of MMB aggregates vs. incubation time, respectively. For the investigated concentration of thrombin (2 nM), the aggregate area saturated after approximately 6 hr.

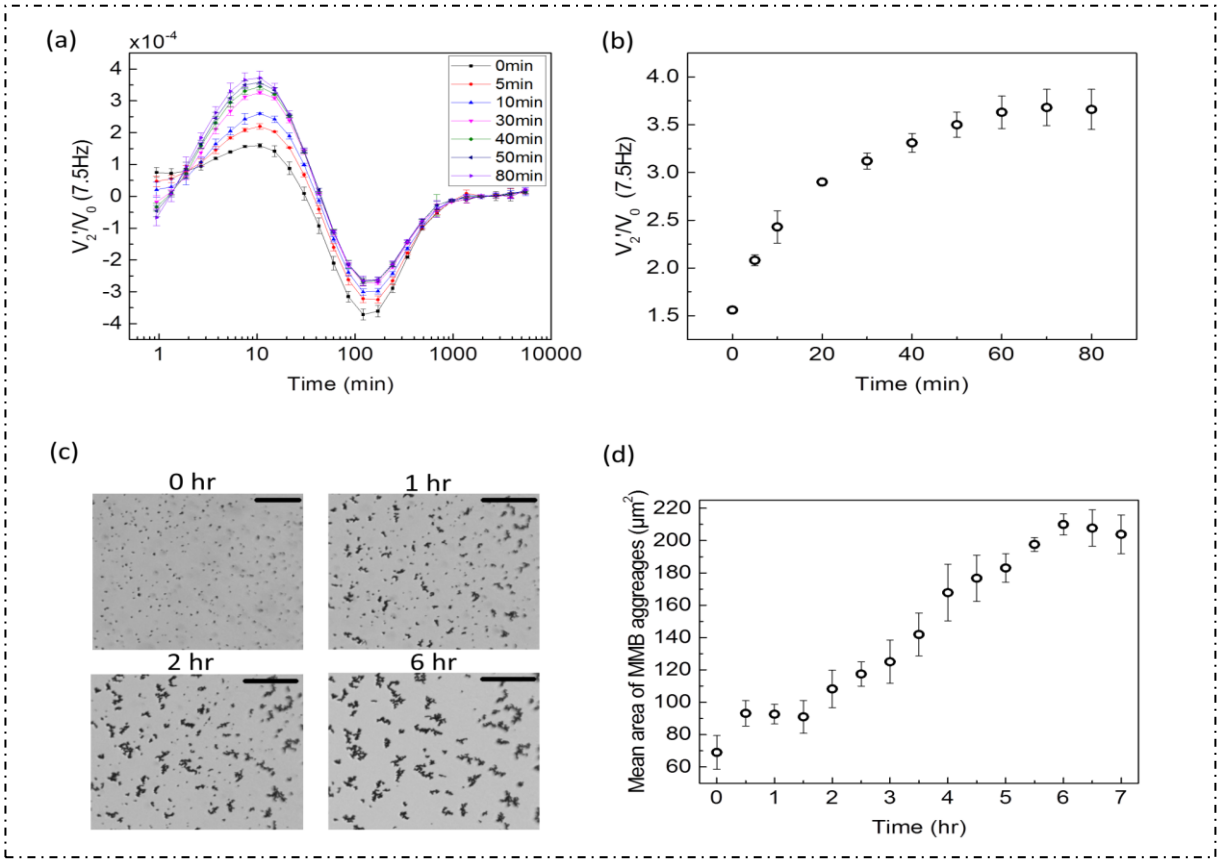

Fig. 2. Results vs. time without magnetic incubation for incubation of aptamer functionalized MBs with 2 nM of thrombin. (a) Optomagnetic spectra (V_2'/V_0 vs. f) at different time points. Occurrence of a signal at low frequencies indicates formation and growth of MNB aggregates. (b) Low-frequency signal $V_2'/V_0\,(7.5\,\mathrm{Hz})$ vs. incubation time. (c) oCelloScope images of aggregation state obtained after the indicated incubation times (all images are shown in Supplementary Material Section S4). (d) Mean area of MMB aggregates vs. incubation time. Error bars indicate standard deviation obtained from triplicate measurements. Scale bars indicate 60 μm

The time-lapse analysis using the two methods confirmed that the MNBs aggregated much faster than the MMBs due to their shorter diffusion time (Gundersen and Palmer, 2007). However, the times needed for both assays were still prohibitively long from a POC application perspective. In this regard, effective manipulation of the aggregate formation by magnetic field can speed up the aggregation resulting in faster detection as well as a lower limit of detection (Antunes *et al.*, 2015; Ranzoni *et al.*, 2012; Baudry *et al.*, 2006). Thus, we designed our incubation strategy for further experiments as 10 min incubation at RT followed by 5 min of magnetic incubation cycles.

3.2 Optomagnetic study with magnetic incubation

For a quantitative analysis of MNB-based assay involving magnetic incubation, we performed an optomagnetic study of six samples with thrombin concentrations ranging from c = 0 (blank) to c = 2 nM (2000 pM). Fig. 3a shows the in-phase part of the normalized optomagnetic spectra (V_2'/V_0 vs. f) measured after magnetic incubation for samples with the indicated thrombin concentrations. From Fig. 3a it is observed that due to the formation of MNB aggregates, higher thrombin concentrations caused an increase of the peak value of the signal as well as a shift of the peak to lower frequencies.

A dose-response curve (Fig. 3b) was obtained by measuring the V_2'/V_0 value at f = 7.5 Hz corresponding to the position of the peak in the spectra for lower thrombin concentrations. From the dose-response curve, we found a limit of

detection (LOD) of 25 pM. This value was obtained from the signal level corresponding to the mean value of the blank signal plus three times its standard deviation.

Compared to the time-lapse analysis without magnetic incubation, the magnetic incubation reduced the required time to form effective clusters by 35 min. In addition, comparing Figs. 2a and 3a, it is observed that the magnetic incubation shifted the frequency of the peak for c = 2 nM from f = 10 Hz to 2.66 Hz. This indicates that the magnetic incubation resulted in the formation of larger clusters than without magnetic incubation. Furthermore, comparing Figs. 2b and 3b, the amplitude of the signal at 7.5 Hz increased a factor of about 7 from 3.5×10^{-4} to 2.6×10^{-3}. Thus, the magnetic incubation also provided a significant signal enhancement.

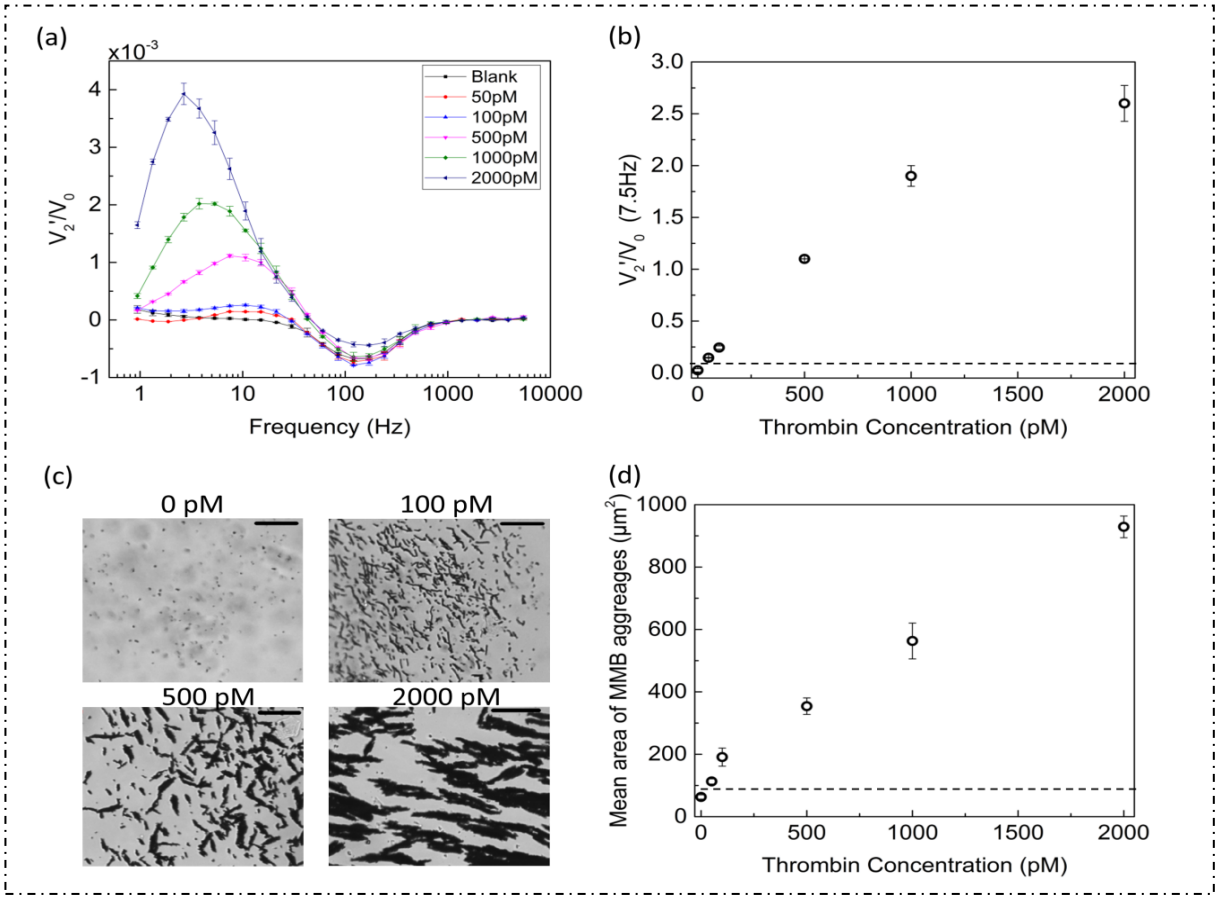

Fig. 3. Results vs. indicated concentrations c of thrombin buffer when magnetic incubation is performed. (a) In-phase optomagnetic spectra of MNBs. (b) Corresponding values of $V_2'/V_0\,(7.5\,\mathrm{Hz})$ *vs. c. (c) oCelloScope images of four different MMB samples (full set of images is given in Supplementary Material Section S4). (d) Corresponding mean area of MMB aggregates vs. c. The black dotted lines in (b) and (d) represent the mean blank signal plus the 3 times of its standard deviation, which is used for calculating the LODs. Error bars are standard deviations obtained from triplicate measurements. Scale bars indicate 60 μm*

3.3 Optical imaging study

For a quantitative analysis of the MMB-based assay, we performed optical imaging study for the same concentrations as studied above after performing the magnetic incubation procedure. Fig. 3c shows the images of the MMB clusters scanned by the oCelloScope for the four indicated values of c. The images clearly illustrate that higher values of c resulted in formation of larger clusters. The blank sample showed very little or no aggregation of the MMBs, whereas the sample with c = 2000 pM showed very large MMB aggregates.

Using the optical sectioning principle, the scanning created multiple stacks of images and from the image stack, the instrument software created stracks of each scanned aggregate, which facilitated calculation of the average projected

area of each aggregate. This was averaged over all MMB aggregates to obtain the mean aggregate area of the population of MMB aggregates (detailed information in Supplementary Material Section S4). Fig. 3d shows this mean area of MMB aggregates vs. *c*. From this dose-response curve, we found an LOD of 25 pM, which is the same value as obtained using the optomagnetic readout.

We have maintained a level of statistical analysis of our experimental results similar to other comparable studies (Yang *et al.*, 2016; Donolato *et al.*, 2015; Hecht *et al.*, 2013). In order to ensure repeatability, all experiments were performed in triplicate. Standard statistical techniques, which take into account the standard deviation (S.D.), e.g., 3×S.D. criterion, were employed to establish the limit of detection of the assay (25 pM). The error bars in Fig. 2 and Fig. 3, representing the standard deviation, are very small compared to the measured signal. This shows the repeatability of the proposed biosensing system.

The images of MMB aggregates for different thrombin concentration in Fig. 3c obtained with magnetic incubation differ significantly from those in Fig. 2c obtained without magnetic incubation. With magnetic incubation, the MMBs formed a tightly packed elongated structure due to the applied magnetic force and torque, whereas without magnetic incubation, the MMBs formed branched clusters. Moreover, comparing Figs. 2d and 3d, it is observed that the magnetic incubation protocol reduced the time to form effective aggregates of the MMBs from about 6 hrs to 15 min while the average area of the aggregates increased by a factor of 4.4 from 209.9 μm^2 to 928.9 μm^2. This also indicates that the magnetic incubation protocol with cycles of magnetic field application and mixing by shaking enabled strong interaction both between MMBs and between the MMBs and the target molecules. Furthermore, as no magnetic field was applied during the shaking step, this step promoted disruption of unspecific bindings between MMBs.

4. Conclusion

We have presented a centrifugal microfludics platform for aptamer-based protein detection in solution by use of magnetic nano- and microbeads. The biosensor can be applied to agglutination assays based on magnetic nanobeads or magnetic microbeads to detect other clinically significant target molecules that have affinity towards certain aptamers. The results presented here illustrate the potential of a compact lab-on-a-disc agglutination assay facilitating automation, low sample volume (10 µl) and a short sample-to-answer time. The integration of the assay in a microfluidic disc enabled the automation of sample handling, mixing and magnetic incubation, which play a major role in increasing reliability and repeatability of the assay as well as for the user-friendliness of the technique. The optomagnetic readout using the Blu-ray OPU and the photodetector produced results on magnetic nanobeads that correlated well with those obtained on magnetic microbeads using direct real-time imaging in the oCelloScope. Thus, these two methods support each other for the usage of small and large particles for a particular assay and further validation of assay. Further, the magnetic incubation protocol significantly shortened the aggregate formation time and enhanced the size of the aggregates such that these were detectable by the two readout techniques for low concentrations of thrombin. In addition, although MMBs require much more time than MNBs to form aggregates by diffusion, the magnetic incubation facilitated detectable aggregation for both bead sizes with the same LODs and the same total assay time. In future study, we will extend our current work to more complex sample matrices, such as blood plasma, where the plasma samples can be obtained via centrifugal separation from a whole blood sample by a simple extension of the presented disc system with no need for user intervention or advanced sample preparation.

Acknowledgements

This work was financially supported by the European Research Council under the European Union's Seventh Framework Programme (FP7/2007-2013) grant no. 320535-HERMES and grant no. 604448-NanoMag. The authors also acknowledge the support from the IDUN project (grant no. DNRF122) funded by the Danish National Research Foundation and the Velux Foundations.

References

Andrea Ranzoni, Gwenola Sabatte, Leo J. van IJzendoorn, and M.W.J.P., 2012. One-Step Homogeneous Magnetic Nanoparticle Immunoassay for Biomarker Detection Directly in Blood Plasma. ACS NANO 6, 3134–3141.

Anja Mezger, Jeppe Fock, Paula Antunes, Frederik W. Østerberg, Anja Boisen, Mats Nilsson, Mikkel F. Hansen, Annika Ahlford, and M.D., 2015. Scalable DNA-Based Magnetic Nanoparticle Agglutination Assay for Bacterial Detection in Patient Samples. ACS NANO 9, 7374–7382.

Antunes, P., Watterson, D., Parmvi, M., Burger, R., Boisen, A., Young, P., Cooper, M. a., Hansen, M.F., Ranzoni, A., Donolato, M., 2015. Quantification of NS1 dengue biomarker in serum via optomagnetic nanocluster detection. Scientific Reports 5, 16145. doi:10.1038/srep16145

Baudry, J., Rouzeau, C., Goubault, C., Robic, C., Cohen-Tannoudji, L., Koenig, a, Bertrand, E., Bibette, J., 2006. Acceleration of the recognition rate between grafted ligands and receptors with magnetic forces. Proceedings of the National Academy of Sciences of the United States of America 103, 16076–16078. doi:10.1073/pnas.0607991103

Bejhed, R.S., de la Torre, T.Z.G., Donolato, M., Hansen, M.F., Svedlindh, P., Strömberg, M., 2015. Turn-on optomagnetic bacterial DNA sequence detection using volume-amplified magnetic nanobeads. Biosensors and Bioelectronics 66, 405–411. doi:10.1016/j.bios.2014.11.048

Beyor, N., Seo, T.S., Liu, P., Mathies, R. a., 2008. Immunomagnetic bead-based cell concentration microdevice for dilute pathogen detection. Biomedical Microdevices 10, 909–917. doi:10.1007/s10544-008-9206-3

Bock, L.C., Griffin, L.C., Latham, J.A., Vermaas, E.H., Toole, J.J., 1992. Selection of single-stranded DNA molecules that bind and inhibit human thrombin. Nature 355 (6360), 564-566. doi:10.1038/355564a0

Chen, F. yuan, Wang, Z., Li, P., Lian, H.Z., Chen, H.Y., 2013. Aptamer-based thrombin assay on microfluidic platform. Electrophoresis 34, 3260–3266. doi:10.1002/elps.201300338

Chertok, B., Moffat, B. a., David, A.E., Yu, F., Bergemann, C., Ross, B.D., Yang, V.C., 2008. Iron oxide nanoparticles as a drug delivery vehicle for MRI monitored magnetic targeting of brain tumors. Biomaterials 29, 487–496. doi:10.1016/j.biomaterials.2007.08.050

Choi, J.-W., Oh, K.W., Thomas, J.H., Heineman, W.R., Halsall, H.B., Nevin, J.H., Helmicki, A.J., Henderson, H.T., Ahn, C.H., 2002. An integrated microfluidic biochemical detection system for protein analysis with magnetic bead-based sampling capabilities. Lab on a Chip 2, 27. doi:10.1039/b107540n

Donolato, M., Antunes, P., de la Torre, T.Z.G., Hwu, E.-T., Chen, C.-H., Burger, R., Rizzi, G., Bosco, F.G., Strømme, M., Boisen, A., Hansen, M.F., 2015. Quantification of rolling circle amplified DNA using magnetic nanobeads and a Blu-ray optical pick-up unit. Biosensors and Bioelectronics 67, 649–655. doi:10.1016/j.bios.2014.09.097

El-Boubbou, K., Gruden, C., Huang, X., 2007. Magnetic glyco-nanoparticles: a unique tool for rapid pathogen detection, decontamination, and strain differentiation. Journal of the American Chemical Society 129, 13392–3. doi:10.1021/ja076086e

Fredborg, M., Andersen, K.R., Jorgensen, E., Droce, a, Olesen, T., Jensen, B.B., Rosenvinge, F.S., Sondergaard, T.E., 2013. Real-time optical antimicrobial susceptibility testing. J Clin Microbiol 51, 2047–2053. doi:10.1128/JCM.00440-13

Gonzales, M., Krishnan, K.M., 2005. Synthesis of magnetoliposomes with monodisperse iron oxide nanocrystal cores for hyperthermia. Journal of Magnetism and Magnetic Materials 293, 265–270. doi:10.1016/j.jmmm.2005.02.020

Gu, H., Xu, K., Xu, C., Xu, B., 2006. Biofunctional magnetic nanoparticles for protein separation and pathogen detection. Chemical communications (Cambridge, England) 941–949. doi:10.1039/b514130c

Gundersen, S.I., Palmer, A.F., 2007. Conjugation of Methoxypolyethylene Glycol to the Surface of Bovine Red Blood Cells. Biotechnology and Bioengineering 96, 1199–1210. doi:10.1002/bit

Hecht, A., Commiskey, P., Shah, N., Kopelman, R., 2013. Bead assembly magnetorotation as a signal transduction method for protein detection. Biosensors and Bioelectronics 48, 26–32. doi:10.1016/j.bios.2013.03.073

Horng, H.E., Yang, S.Y., Hong, C.Y., Liu, C.M., Tsai, P.S., Yang, H.C., Wu, C.C., 2006. Biofunctionalized magnetic nanoparticles for high-sensitivity immunomagnetic detection of human C-reactive protein. Applied Physics Letters 88, -. doi:10.1063/1.2207990

Jain, T.K., Richey, J., Strand, M., Leslie-Pelecky, D.L., Flask, C. a., Labhasetwar, V., 2008. Magnetic nanoparticles with dual functional properties: Drug delivery and magnetic resonance imaging. Biomaterials 29, 4012–4021. doi:10.1016/j.biomaterials.2008.07.004

Jenny Göransson, Teresa Zardán Gómez De La Torre, Mattias Strömberg, Camilla Russell, Peter Svedlindh, Maria Strømme, and M.N., 2010. Sensitive Detection of Bacterial DNA by Magnetic Nanoparticles. Analytical Chemistry 82, 9138–9140.

Kwakye, S., Goral, V.N., Baeumner, A.J., 2006. Electrochemical microfluidic biosensor for nucleic acid detection with integrated minipotentiostat. Biosensors & bioelectronics 21, 2217–23. doi:10.1016/j.bios.2005.11.017

Li, Song; Liu, Hongna; Deng, Yan; Lin, Lin; He, N., 2013. Development of a Magnetic Nanoparticles Microarray for Simultaneous and Simple Detection of Foodborne Pathogens. Journal of Biomedical Nanotechnology 9, 1254–1260.

Louis C. Bock, Linda C. Griffin, John A. Latham, E.H.V.& J.J.T., 1992. Selection of single-stranded DNA molecules that bind and inhibit human thrombin. Nature 355, 564–566.

Nam, J.-M., Thaxton, C.S., Mirkin, C. a, 2003. Nanoparticle-based bio-bar codes for the ultrasensitive detection of proteins. Science (New York, N.Y.) 301, 1884–1886. doi:10.1126/science.1088755

Noroozi, Z., Kido, H., Peytavi, R., Nakajima-Sasaki, R., Jasinskas, A., Micic, M., Felgner, P.L., Madou, M.J., 2011. A multiplexed immunoassay system based upon reciprocating centrifugal microfluidics. Review of Scientific Instruments 82, 064303. doi:10.1063/1.3597578

Quan, X., Uddin, R., Heiskanen, A., Parmvi, M., Nilson, K., Donolato, M., Hansen, M.F., Rena, G., Boisen, A., 2015. The copper binding properties of metformin – QCM-D, XPS and nanobead agglomeration. Chem. Commun. 12, 1–4. doi:10.1039/C5CC04321B

Steigert, J., Grumann, M., Brenner, T., Mittenbuhler, K., Nann, T., Ruhe, J., Moser, I., Haeberle, S., Riegger, L., Riegler, J., 2005. Integrated Sample Preparation, Reaction, and Detection on a High-frequency Centrifugal Microfluidic Platform. Journal of the Association for Laboratory Automation 10, 331–341. doi:10.1016/j.jala.2005.07.002

Tasset, D.M., Kubik, M.F., Steiner, W., 1997. Oligonucleotide inhibitors of human thrombin that bind distinct epitopes. Journal of molecular biology 272, 688–98. doi:10.1006/jmbi.1997.1275

Tennico, Y.H., Hutanu, D., Koesdjojo, M.T., Bartel, C.M., Remcho, V.T., 2010. On-chip aptamer-based sandwich assay for thrombin detection employing magnetic beads and quantum dots. Analytical Chemistry 82, 5591–5597. doi:10.1021/ac101269u

Tsai, H.Y., Hsu, C.F., Chiu, I.W., Bor Fuh, C., 2007. Detection of C-reactive protein based on immunoassay using antibody-conjugated magnetic nanoparticles. Analytical Chemistry 79, 8416–8419. doi:10.1021/ac071262n

Wang, L., Gan, X.-X., 2009. Biomolecule-functionalized magnetic nanoparticles for flow-through quartz crystal microbalance immunoassay of aflatoxin B1. Bioprocess and biosystems engineering 32, 109–16. doi:10.1007/s00449-008-0228-2

Wang Z, Fan Y, Chen J, Guo Y, Wu W, He Y, Xu L, F.F., 2013. A microfluidic chip-based fluorescent biosensor for the sensitive and specific detection of label-free single-base mismatch via magnetic beads-based "sandwich" hybridization strategy. Electrophoresis 34, 2177–2185.

Weng, X., Zhao, W., Neethirajan, S., Duffield, T., 2015. Microfluidic biosensor for β-Hydroxybutyrate (βHBA) determination of subclinical ketosis diagnosis. Journal of Nanobiotechnology 13, 1–8. doi:10.1186/s12951-015-0076-6

Wilson, K.S., Goff, J.D., Riffle, J.S., Harris, L. a., St Pierre, T.G., 2005. Polydimethylsiloxane-magnetite nanoparticle complexes and dispersions in polysiloxane carrier fluids. Polymers for Advanced Technologies 16, 200–211. doi:10.1002/pat.572

Wu, S.J., Duan, N., Wang, Z.P., Wang, H.X., 2011. Aptamer-functionalized magnetic nanoparticle-based bioassay for the detection of ochratoxin a using upconversion nanoparticles as labels. Analyst 136, 2306–2314. doi:Doi 10.1039/C0an00735h

Yager, P., Domingo, G.J., Gerdes, J., 2008. Point-of-care diagnostics for global health. Annual review of biomedical engineering 10, 107–44. doi:10.1146/annurev.bioeng.10.061807.160524

Yang, J., Donolato, M., Pinto, A., Bosco, F.G., Hwu, E.-T., Chen, C.-H., Alstrøm, T.S., Lee, G.-H., Schäfer, T., Vavassori, P., Boisen, A., Lin, Q., Hansen, M.F., 2016. Blu-ray based optomagnetic aptasensor for detection of small molecules. Biosensors and Bioelectronics 75, 396–403. doi:10.1016/j.bios.2015.08.062

Yue Zhang, Chalermchai Pilapong, Yuan Guo, Zhenlian Ling, Oscar Cespedes, Philip Quirke, and D.Z., 2013. Sensitive, Simultaneous Quantitation of Two Unlabeled DNA Targets Using a Magnetic Nanoparticle–Enzyme Sandwich Assay. Analytical Chemistry 85, 9238–9244.

Zaytseva, N. V, Goral, V.N., Montagna, R. a, Baeumner, A.J., 2005. Development of a microfluidic biosensor module for pathogen detection. Lab on a chip 5, 805–811. doi:10.1039/b503856a